arXiv:astro-ph/9805093v1 7 May 1998

Discovery of $z = 0.0912$ and $z = 0.2212$ Damped Lyα Absorption Line Systems Toward the Quasar OI 363: Limits on the Nature of Damped Lyα Galaxies[1]

Sandhya M. Rao[2] and David A. Turnshek[3]
Department of Physics and Astronomy, University of Pittsburgh, Pittsburgh, PA 15260

Received _____; accepted _____

[1]Based on data obtained with the NASA/ESA Hubble Space Telescope at the Space Telescope Science Institute, which is operated by the Association of Universities for Research in Astronomy, Inc., under NASA contract NAS5-26555, and on observations made with the KPNO WIYN telescope, National Optical Astronomy Observatories, operated by AURA, Inc., under cooperative agreement with the National Science Foundation.

[2]E-mail: rao@phyast.pitt.edu

[3]E-mail: turnshek@vms.cis.pitt.edu

ABSTRACT

The discovery of a $z_{abs} = 0.0912$ damped Lyα absorption-line system in the HST-FOS ultraviolet spectrum of the quasar OI 363 (0738+313) is reported. This is the lowest redshift quasar damped Lyα system known. Its neutral hydrogen column density is N(H I)$= 1.5 \pm 0.2 \times 10^{21}$ atoms cm^{-2}, which easily exceeds the classical criterion for damped Lyα of N(H I)$\geq 2 \times 10^{20}$ atoms cm^{-2}. Remarkably, a $z_{abs} = 0.2212$ damped system with N(H I)$= 7.9 \pm 1.4 \times 10^{20}$ atoms cm^{-2} has also been discovered in the same spectrum.

In the past, the standard paradigm for damped Lyα systems has been that they arise in galactic or protogalactic H I disks with low impact parameters in luminous galaxies. However, WIYN imaging of the OI 363 field shows that none of the galaxies visible in the vicinity of the quasar is a luminous gas-rich spiral with low impact parameter, either at $z = 0.0912$ or $z = 0.2212$. Thus, these damped systems are among the clearest examples yet of cases that are inconsistent with the standard damped Lyα − HI-disk paradigm.

Subject headings: quasars: absorption lines — quasars: individual (OI 363, 0738+313) — galaxy formation

1. INTRODUCTION

While it is widely recognized that QSO damped Lyα absorption-line systems are important probes of galaxy formation, their utility is hampered by their rarity, especially in the ultraviolet at low redshift. For example, only one damped Lyα line was discovered in the *Hubble Space Telescope* Quasar Absorption Line Key Project (Jannuzi et al. 1998) and, at the present time, only two damped systems have been confirmed from a survey of QSOs with the *International Ultraviolet Explorer* (Lanzetta, Wolfe & Turnshek 1995). In the ultraviolet ($\lambda < 3220$ Å), Lyα absorption has redshifts $z_{abs} < 1.65$. This corresponds to look-back times up to 77% of the age of the Universe for $q_0 = 0.5$. Thus, it is particularly important that low-redshift examples of damped Lyα systems be discovered and studied. This will eventually allow the evolutionary links between H I in nearby galaxies (Rao & Briggs 1993) and the high-redshift damped systems found in optical surveys (Wolfe et al. 1986; Lanzetta et al. 1991; Wolfe et al. 1995) to be explored.

We recently completed a highly successful HST Faint Object Spectrograph program to discover low-redshift ($z < 1.65$) damped Lyα lines in QSO spectra (Turnshek 1997; Rao & Turnshek 1998). Coupled with earlier HST archival work (Rao, Turnshek & Briggs 1995), we have studied the ultraviolet Lyα absorption line in 88 Mg II absorption-line systems. This targeted search has greatly increased the number of known low-redshift damped systems. We currently have 12 damped systems in our sample, including two that were discovered serendipitously in spectral regions without available Mg II information.

In this *Letter*, we report our discovery of the lowest redshift damped Lyα absorption-line system known — a $z_{abs} = 0.0912$ system with neutral hydrogen column density N(H I)$\approx 1.5 \times 10^{21}$ atoms cm^{-2} in the spectrum of the quasar OI 363 (0738+313; $z_{em} = 0.630$). This object has a known Mg II absorption-line system at $z_{abs} = 0.2213$ (Boulade et al. 1987), but no evidence for an absorption system at $z_{abs} = 0.0912$ had ever

been reported prior to our survey. We obtained a HST-FOS G160L/BL spectrum of this object to determine the nature of the Lyα line associated with the $z_{abs} = 0.2213$ system and coincidentally discovered the damped system at $z_{abs} = 0.0912$. Remarkably, the slightly higher redshift system is also damped with N(H I)$\approx 7.9 \times 10^{20}$ atoms cm^{-2}.

In §2 we describe our observations and data analysis. The observations include the HST-FOS spectrum of OI 363 and an R image of the field obtained in seeing of 0.55″ with the WIYN 3.5-m Telescope on Kitt Peak. We find that none of the galaxies visible in the vicinity of the quasar are luminous gas-rich galaxies with low impact parameters, either at $z \approx 0.0912$ or $z \approx 0.2212$. In §3 we discuss these results.

2. OBSERVATIONS AND DATA ANALYSIS

2.1. HST-FOS Spectroscopy

A one-orbit ultraviolet spectrum of OI 363 was obtained on 1996 May 15 with the HST-FOS using the G160L/BL grating-digicon combination and one of the 1.0-PAIR (0.86″ square) apertures. The exposure time was 1520 seconds. The pipeline-processed data were re-sampled to the original dispersion of 1.72 Å per pixel (quarter-diode); the re-sampled spectrum is shown in Fig. 1 along with the 1σ error array. A signal-to-noise ratio of ≈ 10 per resolution element (diode) was measured near 1400 Å in the continuum adjacent to the positions of the wide absorption lines seen in the spectrum.

The most recent calibration and data reduction procedures have been applied to the data as recommended by the HST-FOS STScI analysis team. Pixel numbers 900 through 1199 of the G160L/BL mode have zero sensitivity to dispersed light. These were used to determine a *wavelength-independent* correction for scattered light and background (Kinney & Bohlin 1993 ISR CAL/FOS-103). The average flux value in the zero-sensitivity pixels

was then subtracted from the data during pipeline processing. In addition, the new and improved Average Inverse Sensitivity method of flux calibration was used in the pipeline. The flux in the core of the wide absorption line at ≈ 1330 Å is approximately equal to the 1σ uncertainty in the background. Thus, the marginal non-zero intensity of this wide absorption line may be attributed to the uncertainty in the background measurement. However, the core of the wide absorption line at ≈ 1486 Å is a $\gtrsim 5\sigma$ deviation from zero flux, and this is not expected to be due to uncorrected scattered light, dark counts or red-leak (Ed Smith, FOS Instrument Scientist, private communication).

Because neither of the wide absorption lines has zero flux at its line center, we suspect that there is a background subtraction problem in the FOS G160/BL spectrum (see also Boissé et al. 1998). First, both absorption systems at redshifts 0.0912 and 0.2212 have now been found to be 21 cm absorbers (Lane et al. 1998a; b). For 21 cm absorption to appear the H I column density must always be significantly greater than N(H I)$= 2 \times 10^{20}$ atoms cm^{-2} (Briggs 1988), which is the classical limiting criterion defined in surveys for damped Lyα lines (Wolfe et al. 1986). Simulations at the FOS G160L/BL resolution show that when 21 cm absorption is present, the resulting damped Lyα line should be black, or nearly black, at the line center. Secondly, as discussed below, Voigt damping profiles corresponding to column densities N(H I)$> 2 \times 10^{20}$ cm^{-2} are found to be excellent fits to both wide absorption lines (see Figs. 2 and 3). Thus, the different non-zero flux values at the cores of the two lines suggest that a wavelength-dependent correction for the background is needed. Another possibility is that there is some other UV-bright object in the $0.86''$ FOS aperture that is either unabsorbed or partially absorbed, but our WIYN image of the field clearly indicates that if this is the case, then the object is not visible in R. To confirm the existence of very closely spaced gravitationally lensed components would require better imaging, but we have dismissed this possibility for now.

Given that both absorption systems have also been detected in 21 cm observations, the wide absorption lines are certainly due to Lyα. Their equivalent widths indicate that they lie on the damping part of the curve-of-growth. Their H I column densities were determined as follows: a continuum level (CL1) was selected by eye using data points on either side of the line near 1330Å. Seventeen percent of CL1 was subtracted so that the line center had zero flux, resulting in a new continuum (CL2). The spectrum was then normalized by CL2. Fig. 2 shows a Voigt profile fit to the Lyα line for $z_{abs} = 0.0937$ and N(H I)$= 1.5 \times 10^{21}$ cm^{-2}. Similarly, for the line near 1486Å, 32% of the original continuum was subtracted so that the line center would have zero flux and the spectrum was re-normalized. Fig. 3 shows a Voigt profile fit to this Lyα line for $z_{abs} = 0.2224$ and N(H I)$= 7.9 \times 10^{20}$ cm^{-2}. The parameters that best fit the data were determined by minimizing the least squares difference between the data and the fit within 12Å on either side of the line near 1330Å and within 17Å on either side of the line near 1486Å. The largest uncertainty in the measured column densities comes from continuum placement. An estimate of the uncertainty was determined by placing new continua at levels corresponding to $CL2 \pm 1\sigma$ with the σ offset given by the error array. The spectrum was then re-normalized using the new continua, and the best fit damping profiles were re-determined. The resolution (FWHM) of the observations is approximately one diode, which is 6.6Å. The data were obtained with quarter-substepping so that each pixel is $\approx$ 1.7Å. This suggests that the redshifts of the damped Lyα lines in our G160L/BL spectrum can be determined to an accuracy of $z \approx 0.001$. The associated 21 cm absorption lines have redshifts 0.0912 and 0.2212, which differ by 2.5σ and 1.2σ from the damped line redshifts, respectively. Since the narrow 21 cm line gives a highly accurate measurement of the redshift, the 21 cm measurements are reported as the redshifts of the two systems without error. In summary, the lower redshift damped Lyα line has $z_{abs} = 0.0912$ and N(H I)$= (1.5 \pm 0.2) \times 10^{21}$ cm^{-2}, while the higher redshift line has $z_{abs} = 0.2212$ and N(H I)$= (7.9 \pm 1.4) \times 10^{20}$ cm^{-2}.

2.2. Imaging

Images of the OI 363 field were obtained for us by the KPNO-WIYN Queue team on 1 October 1997 in the Harris R filter using a Tektronics 2048×2048 CCD. The total exposure time was 2700 seconds. The image in Fig. 4 was obtained by bias-subtracting, flat-fielding, registering and combining the original frames in the standard way. The image scale is $0.195''$ per pixel and the seeing was measured to be $0.55''$. The 1σ surface brightness limit is $\mu(R) = 25.4$ magnitudes arcsec^{-2}, while the point source limiting magnitude is $m_R = 25.8$.

In Table 1, we summarize the positions and R-band magnitudes of resolved objects (presumably all galaxies) detected within $40''$ of the quasar and brighter than $R = 24.0$. Objects whose radial light distributions had FWHMs greater than 3.1 pixels, or $0.60''$, were taken to be resolved objects. The positions and R-band magnitudes of all unresolved point sources (presumably stars) that were detected within $40''$ of the quasar are listed in a footnote to Table 1. The cores of the quasar and the objects labeled S5, S10, and S11 are saturated. Since the WIYN frame was uncalibrated, we assumed the magnitude of the star labeled S7 to be $m_R = 18.3$, as measured by Drinkwater et al. (1993) under photometric conditions (see below). We then determined the magnitudes of all the other objects by measuring their intensities relative to S7. Only one object has a measured redshift. The spectrum of the galaxy G11 was obtained for us by Kathy Romer; its redshift is 0.06. It is of interest to consider the possible absolute magnitudes and impact parameters of the other galaxies along the line of sight to OI 363 by assuming that they are at one of the two relevant absorption redshifts. This is done in Table 1. We also give the most likely morphological type for each galaxy as determined either directly from the WIYN image or from its absolute magnitude, as in the case of dwarfs. The implications of these results are discussed in §3.

In addition to our WIYN image, other imaging observations of the OI 363 field have

been discussed in the literature. Le Brun et al. (1993) detected three galaxies with apparent magnitudes $r > 24.5$ within $5.5''$ of the quasar. We detect a marginally significant extended feature to the south-west of the quasar that coincides with one of these detections. We measured 20 counts per pixel above the local background, i.e., a surface brightness of 25.3 magnitudes per square arcsec ($\approx$ the 1σ limit of our image), at the position marked with a cross in Fig. 4. Le Brun et al. suggest that the three galaxies are associated with the quasar and that the galaxy labeled G1 in Table 1 is the one most likely to give rise to the $z_{abs} = 0.2213$ system. However, this conclusion was reached before it was realized that there is a system at $z_{abs} = 0.0912$ and before both systems were recognized to be damped Lyα absorbers. Hutchings & Neff (1990), Drinkwater et al. (1993), and Kirhakos et al. (1994) have also obtained images of OI 363 and the surrounding field. Although the data of Drinkwater et al. (1993) were obtained under photometric conditions, their seeing was only $2.8''$. As a result, they identified galaxy G1 as a star. They also detected two galaxies with reported positions near G2 with magnitudes brighter than our detection limit. These are not visible in our WIYN image.

3. DISCUSSION

The two damped Lyα systems described in this *Letter* provide an excellent opportunity to determine the nature of damped Lyα galaxies. It is interesting to note that none of the objects listed in Table 1 conform to the standard paradigm that damped Lyα galaxies are $M_R^* \approx -21$ spiral disks (Wolfe et al. 1986; Wolfe 1988) with small impact parameters ($b < 20 h_{75}^{-1}$ kpc, Steidel 1995), where we take $B - R = 1$. The usual convention is that this M^* characterizes the Schechter luminosity function of all galaxy types combined (see Fig. 2 in Rao & Briggs 1993). However, the luminosity function of spiral galaxies is best described by a Gaussian function with a peak occurring at $M_R^* \approx -18$ (see Fig. 1 in Rao & Briggs

1993). Interestingly, the fact that brighter spirals have larger H I disks pushes the peak in the interception-probability distribution, which is the product of number density and H I cross-section, to higher luminosities, i.e., to $M_R \approx -21$ (see Fig. 5).

If any one of the faint galaxies reported by Le Brun et al. within $\approx 5''$ of the quasar is the absorber, then it would be an extremely faint dwarf galaxy at $z = 0.0912$, with $M_r \gtrsim -13.5$. On the other hand, the low-surface-brightness feature, marked by a cross in Fig. 4, might be part of a galaxy that lies directly in front of the quasar (in this case for $z = 0.09$, $M_R > -18$ is still likely). Its existence needs to be confirmed. The candidate G1 is a likely absorber at $z = 0.0912$, with absolute magnitude $M_R = -16.9$ ($M_B = -15.9$), ≈ 4 magnitudes fainter than the peak in the interception probability distribution. It is a better candidate at $z = 0.2212$, where it would be brighter and still at a reasonable impact parameter from the quasar. Galaxies G2 through G9 would be dwarfs at both redshifts and, given the high column densities of the two damped Lyα lines, make highly unlikely absorbers at the listed impact parameters. The galaxy G10 appears to be an early type galaxy and, though reasonably bright, is not expected to contain much gas, especially at large impact parameters. The galaxy G11 is the only large spiral in the field (see the Fig. 4 caption); but its redshift is $z = 0.06$ (§2.2). Thus, one could conclude that G1 is the only galaxy that is a reasonable candidate at either absorption redshift.

The absence of luminous spiral galaxy candidates at both damped absorption redshifts represents the most illustrative examples yet of inconsistencies with the standard HI-disk paradigm for damped Lyα systems. Others have discussed similar findings in systems of higher redshift (Steidel et al. 1994; Steidel et al. 1997; Le Brun et al. 1997), but our upper limits on the luminosity of candidate damped Lyα galaxies are about an order of magnitude lower than previous results. Clearly, not all damped Lyα absorbers are luminous spirals.

It has been known for some time that Ω_{gas} at high-redshift is comparable to the

present-day luminous (stellar) cosmological mass density (Rao & Briggs 1993). Thus, the high-redshift damped systems are possibly the progenitors of all present-day galaxies, not just luminous spiral HI-disks. The recent work of Khersonsky & Turnshek (1996), Pettini et al. (1997), Rao & Turnshek (1998), and references therein also reveal problems with this scenario. In fact, the results of our recent survey for damped Lyα absorption at $z_{abs} < 1.65$ indicate that the cosmological mass density of neutral gas, $\Omega_{gas} = 1.3\Omega_{HI}$, at $z \approx 1$ is also comparable to the luminous mass density at the current epoch (Rao & Turnshek 1998). One solution might be the existence of many unrecognized low-surface-brightness (LSB) galaxies or dwarf galaxies at low redshift. However, Briggs (1997a; b) and Zwaan et al. (1997) have concluded that the present-day population of LSB galaxies contributes little to the H I mass density at $z = 0$. They appear to be drawn from the same population as the "normal" high-surface-brightness (HSB) galaxies that are found in optical surveys. Moreover, Bothun et al. (1997) have shown that the average H I column density in LSB galaxies is lower than that in HSB galaxies. Rao & Briggs (1993) used *available data* to show that the local H I mass density and cross-section is dominated by the large spirals. Thus, based on the present imaging results, we conclude that the nature of the damped Lyα galaxies is not yet fully understood.

ACKNOWLEDGEMENTS. We thank Ed Smith and Alex Storrs of the HST-FOS team for help and advice with FOS data reduction. We also thank Diane Harmer and Paul Smith for their assistance in obtaining the WIYN data, and Kathy Romer for kindly obtaining the spectrum of the $z = 0.06$ galaxy (G11) in the field of the quasar OI 363 with the KPNO 4m. This observation allowed us to exclude that galaxy as a possible site for the absorption. We especially thank Eric Monier for his assistance with many aspects of this work.

REFERENCES

Boissé, P., Le Brun, V., Bergeron, J., & Deharveng, J.-M. 1998, A&A, in press

Bothun, G., Impey, C., & McGaugh, S. 1997, PASP, 109, 745

Boulade, O., Kunth, D., Tytler, D., & Vigroux, L. 1987, in High Redshift and Primeval Galaxies, eds. J. Bergeron et al. (France: Edit. Front.), 349

Briggs, F. H. 1988, in QSO Absorption Lines: Probing the Universe, ed. J. C. Blades, D. A. Turnshek, & C. A. Norman (Cambridge: Cambridge Univ. Press), 275

Briggs, F. H. 1997a, ApJ, 484, L29

Briggs, F. H. 1997b, ApJ, 484, 618

Drinkwater, M. J., Webster, R. L., & Thomas, P. A. 1993, AJ, 106, 848

Hutchings, J. B., & Neff, S. G. 1990, AJ, 99, 1715

Jannuzi, B. T., et al. 1998, ApJS, in press

Khersonsky, V. K., & Turnshek, D. A. 1996, ApJ, 471, 657

Kirhakos, S., et al. 1994, PASP, 106, 646

Lane, W., Smette, A., Rao, S. M., Briggs, F., Turnshek, D. A., & Meylan, G. 1998a, ApJ, in press

Lane, W., et al. 1998b, in preparation

Lanzetta, K. M., Wolfe, A. M., Turnshek, D. A., Lu, L., McMahon, R. G., & Hazard, C. 1991, ApJS, 77, 1

Lanzetta, K. M., Wolfe, A. M., & Turnshek, D. A. 1995, ApJ, 440, 435

Le Brun, V., Bergeron, J., Boissé, P., & Christian, C. 1993, A&A, 279, 33

Le Brun, V., Bergeron, J., Boissé, P., & Deharveng, J. 1997, A&A, 321, 733

Pettini, M., Smith, L., King, D., & Hunstead, R. 1997, ApJ, 486, 665

Rao, S. M., & Briggs, F. H. 1993, ApJ, 419, 515

Rao, S. M. 1994, Ph.D. Thesis, University of Pittsburgh

Rao, S. M., Turnshek, D. A., & Briggs, F. H. 1995, ApJ, 449, 488

Rao, S. M., & Turnshek, D. A. 1998, in preparation

Steidel, C. C., Pettini, M., Dickinson, M., & Persson, S. E. 1994, AJ, 108, 2046

Steidel, C. C. 1995, in QSO Absorption Lines, ed. G. Meylan (Berlin: Springer), 139

Steidel, C. C., Dickinson, M., Meyer, D. M., Adelberger, K. L., & Sembach, K. R. 1997, ApJ, 480, 568

Turnshek, D. A. 1997, in Structure and Evolution of the Intergalactic Medium from QSO Absorption Line Systems, eds. P. Petitjean and S. Charlot (France: Edit. Front.), 263

Wolfe, A. M., Turnshek, D. A., Smith, H. E., & Cohen, R. D. 1986, ApJS, 61, 249

Wolfe, A. M., 1988, in QSO Absorption Lines: Probing the Universe, ed. J. C. Blades, D. A. Turnshek and C. A. Norman (Cambridge: Cambridge Univ. Press), 297

Wolfe, A. M., Lanzetta, K. M., Foltz, C. B., & Chaffee, F. H. 1995, ApJ, 454, 698

Zwaan, M. A., Briggs, F. H., Sprayberry, D., & Sorar, E. 1997, ApJ, 490, 173

This manuscript was prepared with the AAS LaTeX macros v4.0.

Fig. 1.— HST-FOS G160L/BL spectrum of the QSO OI363 with damped Lyα absorption lines at 1330Å and 1486Å. The 1σ error array is also shown.

Fig. 2.— Theoretical Voigt profile with redshift $z = 0.0937$ and neutral hydrogen column density $N(HI) = 1.5 \times 10^{21}$ atoms cm^{-2} fit to the absorption line at 1330Å. The normalized continuum and zero levels are shown.

Fig. 3.— Theoretical Voigt profile with redshift $z = 0.2224$ and neutral hydrogen column density $N(HI) = 7.9 \times 10^{20}$ atoms cm^{-2} fit to the absorption line at 1486Å. The normalized continuum and zero levels are shown.

Fig. 4.— A $1.5' \times 1.5'$ field of the WIYN image around the quasar OI 363. North is up and East is to the left. The plate scale is $0.195''$ per pixel. The redshift of the galaxy marked G11 is $z = 0.06$; the expected appearance of a luminous gas-rich spiral at $z = 0.09$ is qualitatively similar to G11.

Fig. 5.— The contribution of spiral and irregular galaxies to the H I absorption cross-section for $N(HI) > 10^{19}$ cm^{-2} at the current epoch assuming a Gaussian luminosity function for spirals and a Schechter luminosity function for irregulars (see Rao & Briggs 1993). The peak in the spiral distribution function occurs at $M_B \approx -20$, or $M_R \approx -21$ assuming $B - R = 1$. See Rao (1994) for details of the luminosity−diameter relations.

Table 1

Extended Sources within 40″ of the Quasar[a]

Object	$\Delta\alpha(''$)	$\Delta\delta(''$)	$\Delta\theta(''$)	m_R[b]	b[c](kpc) (z=0.0912)	M_R[c]	b[c](kpc) (z=0.2212)	M_R[c]	Morphology
G1	2.0	−5.3	5.7	20.8	8.9	−16.9	17.7	−18.8	?
G2	−10.9	3.1	11.3	23.4	17.7	−14.3	35.0	−16.0	dw
G3	7.2	−9.0	11.5	23.7	18.0	−14.0	35.7	−15.9	dw
G4	−10.3	8.8	13.5	22.5	21.1	−15.2	42.2	−17.1	dw
G5	8.4	−11.3	14.1	24.0	22.1	−13.7	43.7	−15.6	dw
G6	9.8	12.1	15.5	22.0	24.3	−15.7	48.1	−17.6	dw
G7	−2.1	17.6	17.7	22.4	27.7	−15.3	54.9	−17.2	dw
G8	−18.9	10.9	21.8	23.3	34.1	−14.4	67.6	−16.3	dw
G9	6.8	21.1	22.1	23.9	34.6	−13.8	68.5	−15.7	dw
G10	−26.5	−9.2	28.1	19.8	44.0	−17.9	87.1	−19.8	early type
G11[d]	31.4	1.2	31.4	17.1					spiral
G12	−25.4	18.9	31.6	22.2	49.5	−15.5	98.0	−17.4	dw
G13	−30.4	11.1	32.4	22.2	50.7	−15.5	100.4	−17.4	dw
G14	−7.6	33.9	34.8	22.5	54.5	−15.2	107.9	−17.1	dw
G15	−31.8	17.2	36.2	22.0	56.7	−15.7	112.2	−17.6	dw

[a]Point sources (Object, $\Delta\alpha(''$), $\Delta\delta(''$), m_R): QSO, 0.0, 0.0, sat; S1, 2.0, 1.5, 20.8; S2, −7.2, 5.3, 22.6; S3, −0.9, 11.5, 20.5; S4, −8.0, 9.8, 20.5; S5, −12.8, 6.0, sat; S6, −17.9, 3.3, 23.4; S7, 3.3, −19.9, 18.3; S8, −17.9, 14.2, 23.4; S9, 11.1, 21.7, 21.3; S10, 5.3, 24.2, sat; S11, −34.7, −11.3, sat.

[b]R-band magnitude of S7 from Drinkwater et al. (1993).

[c]$H_0 = 75$ km s^{-1} Mpc^{-1}, q_0=0.5.

[d]The redshift of galaxy G11 is $z = 0.06$.

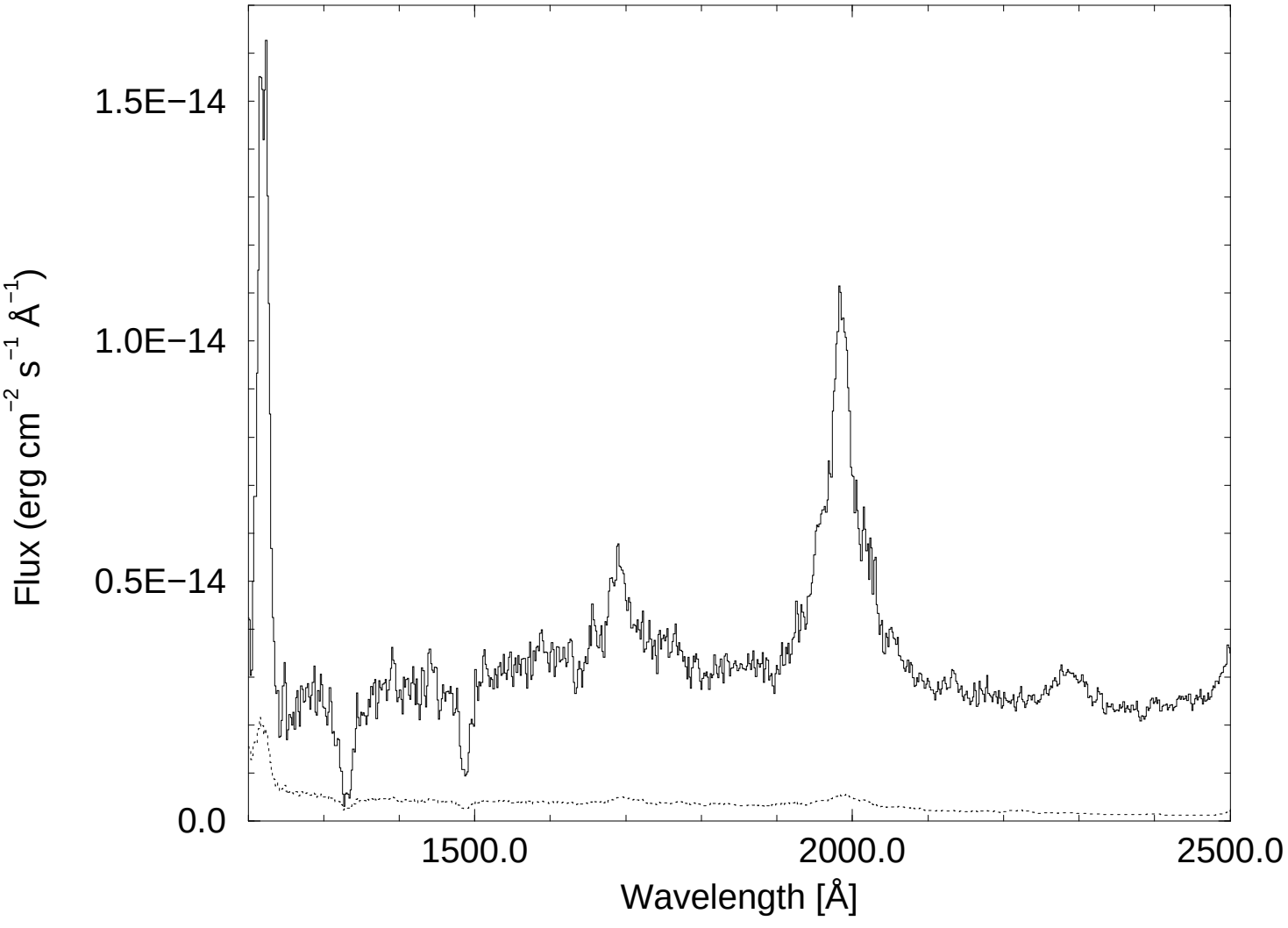
1.5E−14
1.0E−14
0.5E−14
0.0
Flux (erg cm^{-2} s^{-1} Å^{-1})
1500.0
2000.0
2500.0
Wavelength [Å]

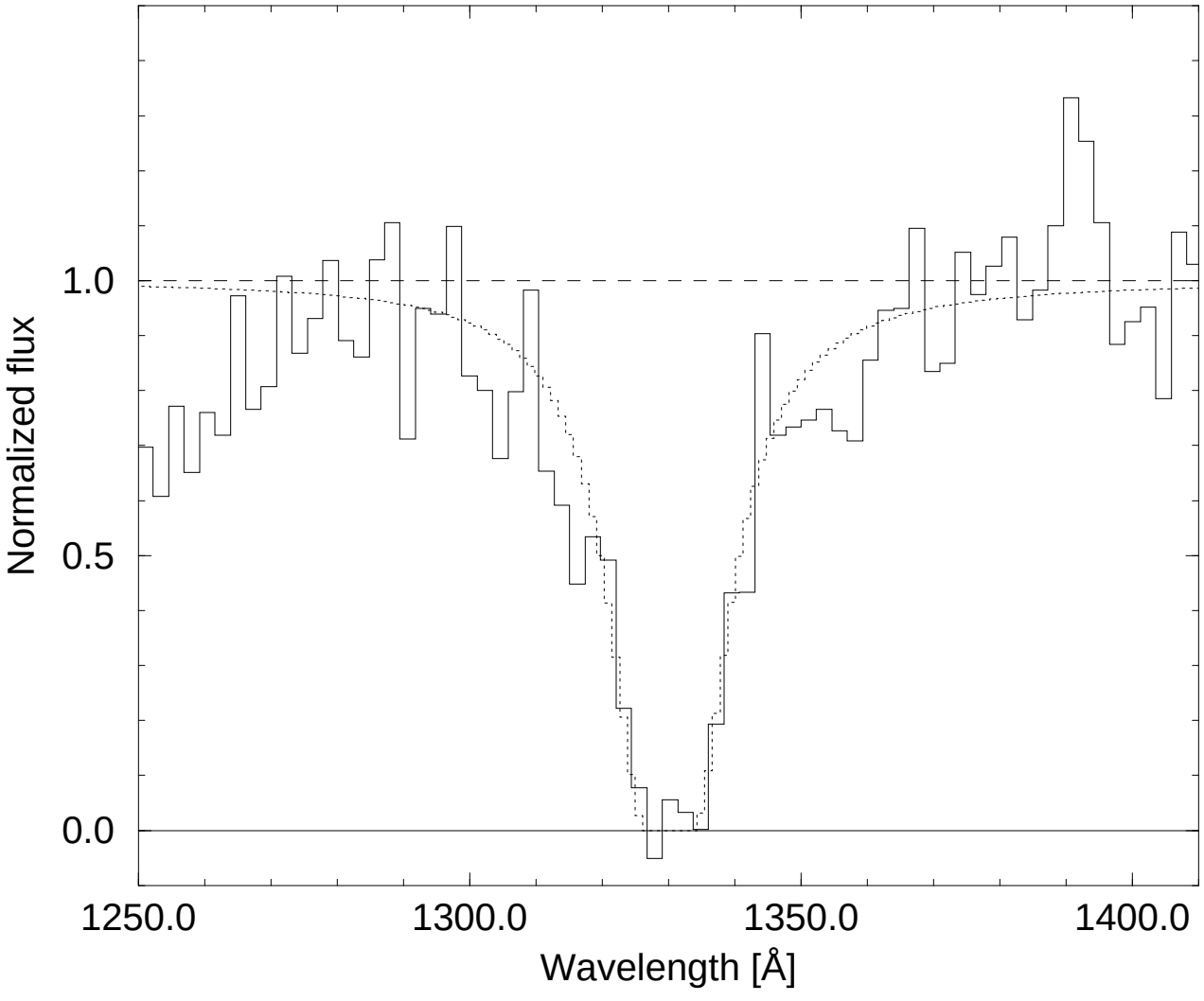
Normalized flux
1.0
0.5
0.0
1250.0
1300.0
1350.0
1400.0
Wavelength [Å]

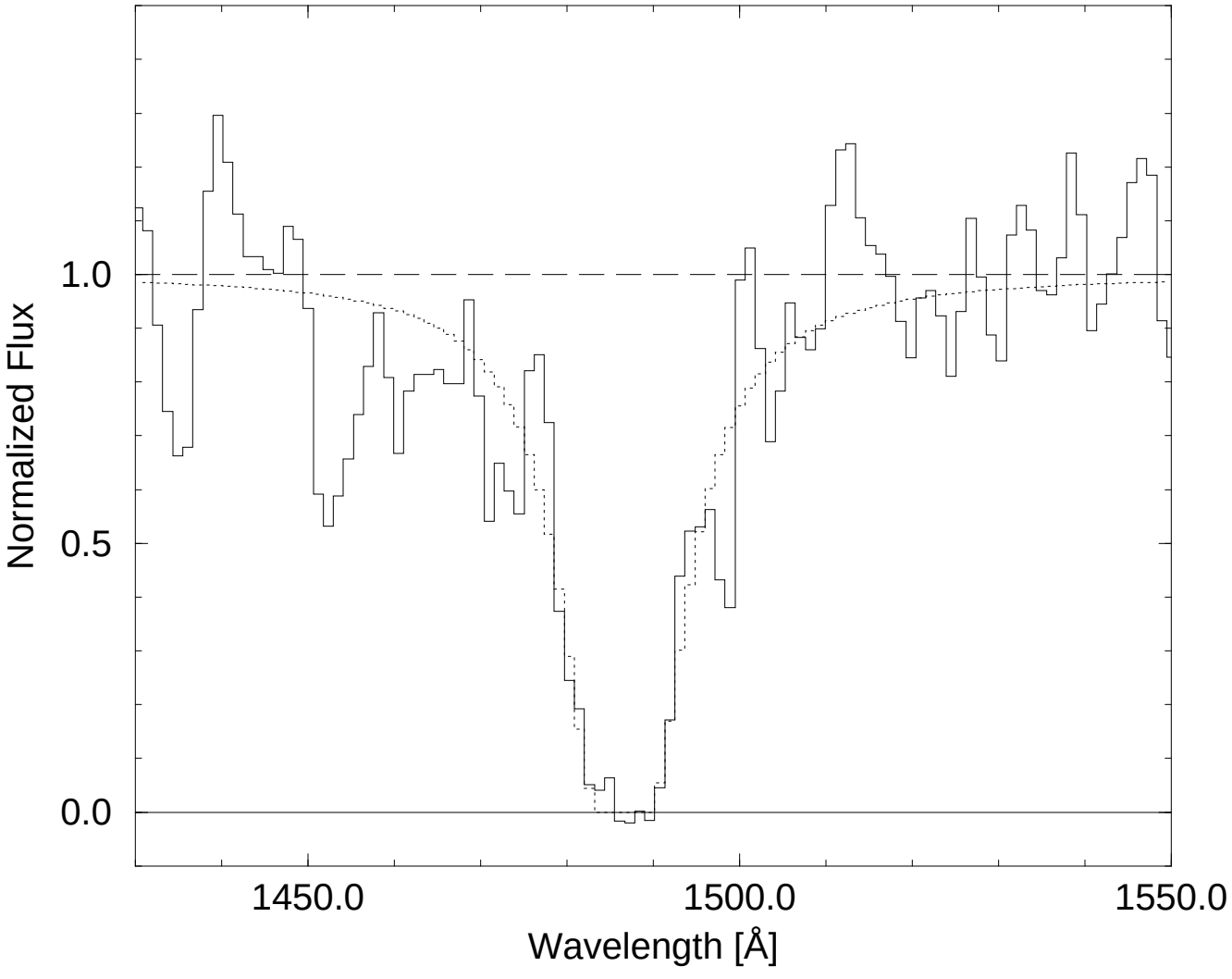
Normalized Flux
1.0
0.5
0.0
1450.0
1500.0
1550.0
Wavelength [Å]

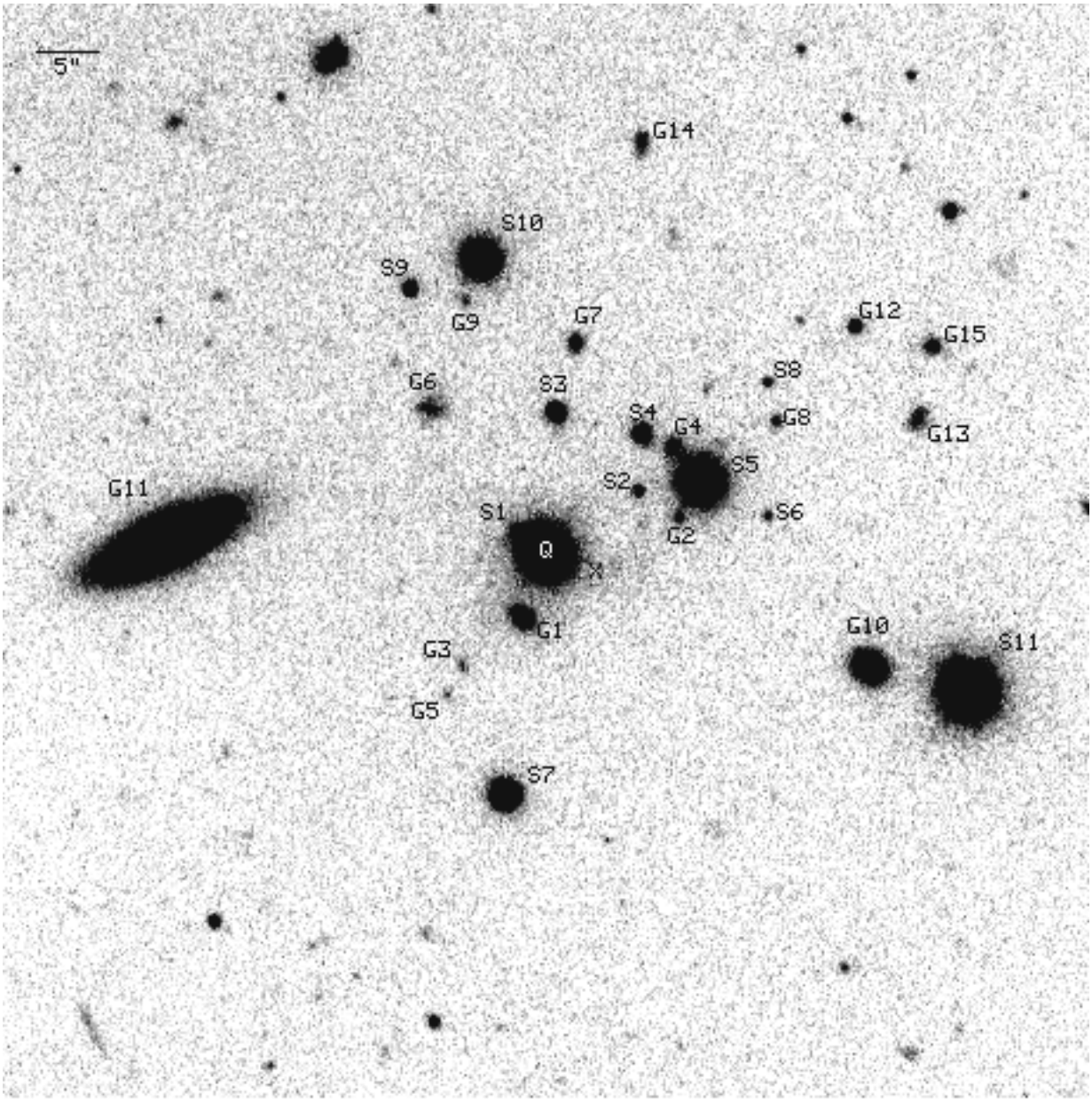
5"
G14
S10
S9
G9
G7
G12
G15
G6
S3
S8
S4
G4
G8
G13
S5
G11
S2
S1
G2
S6
Q
X
G1
G10
S11
G3
G5
S7

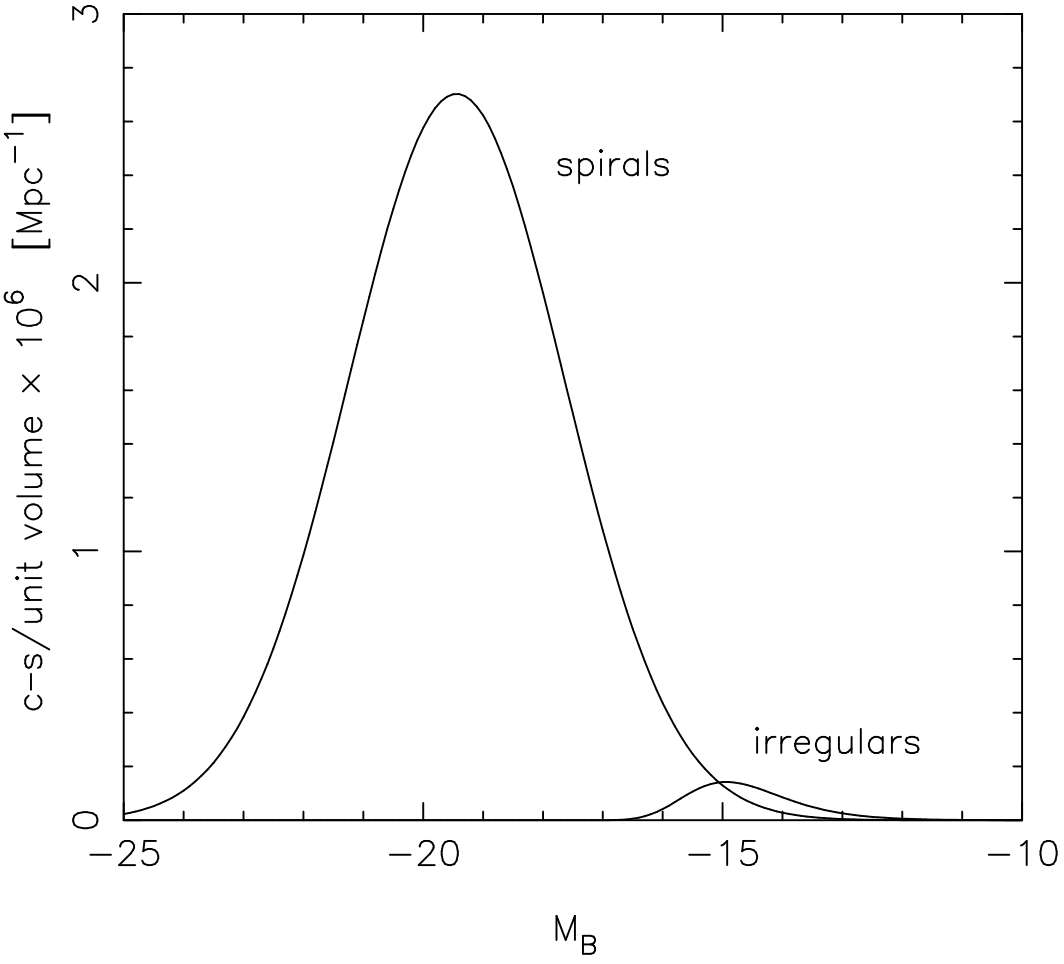
c–s/unit volume x 10^6 [Mpc^{-1}]
0
1
2
3
spirals
irregulars
−25
−20
−15
−10
M_B